Propellants, Explosives, Pyrotechnics, Volume 47, Issue 1, Paper number e202100142
DOI:10.1002/prep.202100142

Styrene-ethylene/butylene-styrene (SEBS) block copolymer binder for solid propellants

Peter J Wilkinson,*[a] Matthew C Weaver,[a] Guillaume Kister[a] and Philip P Gill[a, b]

Abstract: Currently solid composite propellants are manufactured using bespoke, specially manufactured binders. This adds significant cost and obsolescence risks to their development and manufacture. This paper reports on the production of two composite propellants made from a commercially-available-off-the-self polymer as binder by means of a resonant acoustic mixer (RAM) slurry process. The binder consisted of thermoplastic elastomer styrene-ethylene/butylene-styrene (SEBS) block copolymer and the solid filler, either ammonium perchlorate (AP) or 1,3,5-Trinitro-1,3,5-triazinane (RDX). Thermodynamic code demonstrated that SEBS-based propellants exhibited similar theoretical ballistic performance to conventional HTPB-based propellants. Chemical compatibility between SEBS and the solid fillers was shown by the differential scanning calorimetry (DSC) and vacuum stability methods. The novel combination of RAM and slurry coating process produced a propellant moulding powder that was then consolidated by remote hot pressing to simulate an industrial extrusion or rolling process. The propellants exhibited as expected explosive hazard properties and their thermal analysis by DSC-TGA showed typical oxidizer behaviour between AP and SEBS, characterised by two decomposition exotherms (also reported in AP/HTPB compositions), and little or no interaction between RDX and SEBS. The apparent activation energy for decomposition for AP/SEBS (84/16 % w/w) propellant was similar to that for AP/HTPB propellants. This work demonstrates the viability of using SEBS polymer as a binder for solid propellants. The development of propellants using commercially off the shelf, thermoplastic elastomeric binders could add significant benefits in waste reduction through recycling, security of supply, and manufacturing costs.

Keywords: Solid propellants, Formulation, Thermoplastic elastomer, Resonant Acoustic Mixing, LabRAM

1 Introduction

Conventional propellants, nitro-cellulose (NC) based and ammonium perchlorate (AP) composite propellants have been in development for well over five decades. To produce a propellant as economically as possible, the materials required should be of low cost and readily available with a consistent supply. Bespoke binders specially manufactured for propellants increase this cost dramatically, especially in developing a new propellant.

Rubbery composite propellants are the most common type of solid rocket propellant used today[1]. These are made by forming a thermosetting polymer, by far the most common are polyurethanes. Modern polyurethane binders are made by starting with a polymer and forming urethane cross-linkages. The most widely used composite propellant being cured hydroxyl-terminated polybutadiene (HTPB), which is manufactured from hydroxyl-terminated polybutadiene prepolymer cured with an isocyanate. Other prepolymers can be used in a similar manner to form composite propellants. Carboxyl terminated polybutadiene (CTPB) has a similar structure to HTPB, but with the hydroxyl groups replaced by carboxyl groups. Poly(butadiene-acrylic acid-acrylonitrile) (PBAN) is another carboxyl containing prepolymer. Both CTPB and PBAN are cured using with epoxides or aziridines, as opposed to isocyanates[1].

The economic, environmental, legislative and safety factors are crucial in the success of a new propellant. Creating a new propellant with commercially available off the shelf (COTS) polymer as a binder, would be a cost-effective approach. In terms of safety, the binder would need to be a rubbery, elastomeric material. To reduce the environmental impact of disposal of unused munitions, using a thermoplastic elastomer (TPE) as a binder would make a propellant with the potential to be recyclable.

The general feature of all TPEs is that they contain polymer chains which are 'held together' at their working temperature. But when they are heated up this cross-linking becomes ineffective (fugitive) and the chains are able to move, enabling the polymer to flow (a thermoplastic). On cooling these cross-links reform and the polymer regains its rubbery properties[2].

The top five types of industrial mixing technologies are ribbon, tumble, planetary, centrifugal, and Resonant Acoustic® Mixing (RAM)[3]. For the highly solid loaded viscous formulations typical of composite propellants the planetary mixer with its high shear mixing through the use of paddles and blades are historically most commonly used. The resonant acoustic mixer (RAM), manufactured by Resodyn, is a new type of mixer incorporating a mixing vessel attached to a vibrating plate. The RAM mixer generates a uniform shear field throughout the mixing vessel by

---

[a] *P. J. Wilkinson, M. C. Weaver, G. Kister, P. P. Gill*
Centre for Defence Chemistry, Cranfield University, Defence Academy of the United Kingdom, Shrivenham, SN6 8LA, UK
**E-mail: p.wilkinson@cranfield.ac.uk*

[b] *P. P. Gill*
ROXEL (UK Rocket Motors) Ltd, Summerfield Ln, DY11 7RZ, UK

Supporting information for this article is available on the WWW under http://www.pep.wiley-vch.de oscillating the vibrating plate at moderate frequency (ca. 60 Hz) and relatively large displacement (14 mm). The mixer can apply a high level of G-force, up to 100 G, without the use of impellers. The frequency is continually adjusted to stay at the resonant frequency of the mechanical system, maintaining the highest efficiency[4]. According to Resodyn[5,6], the RAM mixer is well suited for propellant mixing. Citing faster mixing times (10 to 100 times faster), the ability to mix in the end-use container and mixing solids in very viscous liquids (up to 350 000 cP end mix viscosity). Additionally, it is claimed that the process is directly scalable.

The use of the RAM mixer may have several advantages over a traditional mechanical mixer in this process. The mixer does not require any impellers or baffles to operate, this reduces the regions where the polymer may be deposited onto the equipment surface. The mixing is also more generalised throughout the mixing vessel, as opposed to being localised around impellers or baffles. It is reported[7] that the RAM mixer is more efficient and quicker at creating a 'well-mixed' mixture, it is thought that this would assist in an even coating of the filler.

A novel method of manufacture using RAM was developed based on a slurry process[8]. The oxidiser crystal is added to a non-solvent and mixed to form a slurry. The polymer binder is dissolved into a solvent and introduced to the slurry. The mixture is then heated and a vacuum or air sweep applied to remove the solvent, leaving the polymer to coat the oxidiser crystals. The slurry is then filtered, washed and dried. The moulding powder can then be compacted by several methods. The simplest is for the moulding powder to be pressed, rolled or extruded, often done at a raised temperature and very high load, often with vacuum applied.[9]; [10]; [11].

This research seeks to evaluate the feasibility of the block copolymer Styrene-ethylene/butylene-styrene (SEBS) as a recyclable COTS binder for a composite propellant. Resonant acoustic mixing is used a method for manufacture of this propellant.

2 Experimental Section

2.1 Materials

Polystyrene-block-poly(ethylene-ran-butylene)-block-polystyrene (SEBS) from Sigma-Aldrich, product number: 200565, CAS number: 66070-58-4, >99 % m/m purity, styrene 29 % w/w, average M_w ~89,000 Daltons by Gel Permeation Chromatography (GPC). Ammonium perchlorate (AP) of nominal particle size 200 µm (AP200) and 90 µm (AP90) respectively, from The Falcon Project Ltd. 1,3,5-Trinitro-1,3,5-triazinane (RDX), type A, class 5 (97+ % pass through a 45 µm sieve) also from QinetiQ plc. Caster and Icing sugar from Tate and Lyle. Toluene, Methyl Ethyl Ketone (MEK), isopropanol (IPA) and dichloromethane (DCM) from Fisher Scientific as extra pure, SLR grade.

2.2 Performance modelling

Theoretical performances of AP/SEBS and RDX/SEBS propellants were calculated using the ICT thermodynamic code, version 1.00, supplied by the Fraunhofer Institute for Chemical Technology. The specific impulse (I_{sp}) was calculated for the rocket propellant formulation of AP/SEBS with a range of theoretical solid loadings (60-98 % w/w) at a pressure ratio of 70:1. Calculations of performance (Force Constant) where calculated for RDX/SEBS (60-98 % w/w) (Figure 2), these were at constant volume yielding force constants, more typical of gun propellants. Both sets of data where compared against the well-known binder of hydroxyl terminated polybutadiene (HTPB).

2.3 RAM slurry Processing

A LabRAM (Resodyn™ Corporation) was used for the propellant mixing. For inert mixes, a stainless steel mixing pot (48 x 48 mm, 80 cm^3) was used, while for propellant mixes, a titanium mixing pot was used (72 x 72 mm, 300 cm^3 internal volume), both fitted with a PEEK lid. These were manufactured in-house following designs from the Falcon Project Ltd. A clamshell clamp attached the lid to the mixing pot. The lid was fitted with a latex balloon (to reduced pressure build-up) and connected to a solvent pump by thin vinyl tubing (I.D. 1 mm). The LabRAM was controlled via aftermarket hardware and software supplied by Falcon Project Ltd., which allowed for temperature logging and vacuum control.

The SEBS was first fully dissolved in toluene (20 % w/v) in the mix pot. The filler was then added to the pot and gently stirred with a spatula, ensuring that polymer solution covered the solid. With the lid and balloon the mix pot was fitted to the LabRAM and vibrated at 70 G for 120 s, followed by 30 s at 30 G. After which the anti-solvent isopropyl alcohol (IPA) was pumped into the mixing pot at 30 G. Double the volume of IPA to the volume of toluene was pumped in from 1.5 to 10 cm^3 min^{-1}. Once the correct amount of IPA had been pumped into the mixing pot, the mixture was vibrated for a final 30 s. The mixture was then filtered (Whatman filter No.1) under vacuum and washed with IPA (ca. 100 cm^{-3}) before being dried in a vacuum desiccator for at least 5 h.

The influence of mixing at different G-forces (after the initial 70 G mix) and the rate of addition of the anti-solvent was assessed using inert sugar mixes. These inert mixtures were produced on a 10 g scale with 70 % w/w solid loading.

2.4 Propellant formulations

A range of propellant compositions (moulding powder, 10 g) was made by hand for hazard assessment. A 10 % w/v solution of SEBS in dichloromethane was added to the filler in the correct proportion for the composite. The mixture was stirred using a bone spatula in a nickel crucible, then most of the solvent was evaporated off by heating in a boiling water bath while being hand mixed. The samples were then left for at least 16 hours for the residual solvent to evaporate.

Five different LabRAM propellant formulations were made in small quantities (ca. 30 g) using the commercially available polymer SEBS (see Table 1). Four with Ammonium Perchlorate (AP) as the filler and another with RDX (1,3,5-Trinitro-1,3,5-triazinane). AP/SEBS were made with a typically bimodal mixture of coarse AP (AP200) and fine (AP90) in a 4:3 ratio. While RDX/SEBS used a mono-modal finer class 5 RDX (97+ % pass through a 45 µm sieve).

Table 1. Composition of novel composite SEBS propellants.

Sample	Solids loading (% w/w)		
	AP[a]	RDX[b]	SEBS
AP/SEBS (60/40)	60		40
AP/SEBS (70/30)	70		30
AP/SEBS (80/20)	80		20
AP/SEBS (84/16)	84		16
RDX/SEBS (80/20)		80	20

[a] AP was a typically bimodal mixture[12] of coarse AP (AP200) and fine (AP90) in a 4:3 ratio. [b] class 5 RDX.

All moulding powders (ca. 30 g scale) were pressed using a hydraulic ram (Clarke - Hydraulic 10 Tonne Press) with the sample positioned in a mould on an oil heater plate (made in-house). SEBS propellant were pressed at 125 °C with 5 tonnes of load with a dwell time of 300 s in a mould 55 x 100 mm, with enough material to press to thickness of around 4 mm. It was then cooled under load to 70 °C (approximately 300 s) before sample removal. Two sheets of each formulation were made (Figure 1).

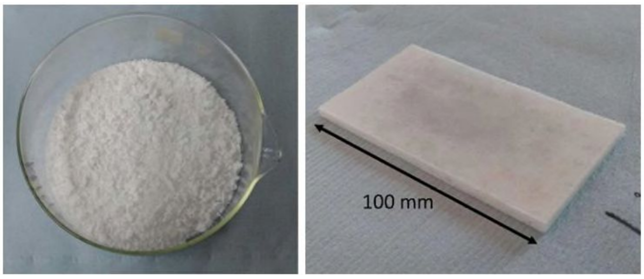

Figure 1. AP/SEBS (84/16) propellant as moulding powder (left) and after pressing (right).

2.5 Experimental Analysis

Densities. True density was determined by helium pycnometer using an AccuPyc 1330 Pycnometer. Pressed propellant samples of about 0.5 g were cut using a razor blade and weighed to 0.1 mg. Hand measurements were used to determine the bulk density of the filled TPEs. Length and width of the whole pressed sheet was measured at least three times to a hundredth of a millimetre using digital callipers and the thickness was measured eight times to one micrometre using a digital micrometer. Tap density (or apparent density) was determined for the moulding powders. About 10 g of sample was poured into a 50 cm^3 measuring cylinder, then dropped from a 32 mm height onto a rubber pad 30 times. The tap density was calculated by dividing the mass (g) by the volume (cm^3) occupied by the powder after consolidation.

Particle size distribution of the moulding powders was measured by sieving. Test sieves (Endecotts) of 0.425 mm, 1 mm and 1.7 mm were used to separate the mixture into different particle size bins. All other particle size analysis was acquired by laser diffraction using a CILAS 1190 particle size analyser. The particle size of RDX was determined in wet mode, by dispersing about 50 mg in water using teepol as a wetting agent, while other samples were determined in dry mode (ca. 10 to 50 g sample size).

Optical microscopy was performed using a Keyence VHX-1000 microscope with VH-Z20R (20 to 200 zoom) and VH-Z250R (250 to 2500 zoom) attachments. Analysis was conducted using the VHX software, version 1.3.0.7. Samples were illuminated from above on a contrasting blue background.

Thermogravimetric analysis - differential scanning calorimetry (TGA/DSC) was performed on a Mettler Toledo TGA/DSC3+ instrument fitted with DSC sensors. Samples (ca. 5 mg) where placed in Mettler Toledo 100 µL aluminium crucibles with no lid. Samples were heated at 10 °C min^{-1} in a nitrogen atmosphere up to 500 °C.

2.6 Compatibility Testing

Differential scanning calorimetry compatibility test: This is test 4 in STANAG 4147 (Edition 2)[13]. Samples were placed in aluminium crucibles and heated from 30 to 550 °C, 2 °C min^{-1} under nitrogen. Thermograms from 2 mg, 1:1 (w/w) sample mixtures were compared to 1 mg of samples of each material tested separately. The peak temperature of the primary decomposition was determined, if this peak temperature reduces by less than 4 °C from separate material to the mixture, the mixture is considered compatible. Additionally, the peak shapes must also be examined for any changes due to interactions between components.

Vacuum stability test: This is test 1 in STANAG 4147 (Edition 2). A 5 g admixture (2.5 g of each material) was sealed in a glass tube under vacuum and kept at 100 °C for 40 h. The gas released was calculated by means of a digital manometer. This was compared to the gas released from 2.5 g of each material separately tested in the same manner. If the admixture releases less than 5 cm^3 of addition gas the mixture is deemed compatible.

2.7 Hazard Testing

Hazard testing was carried out on the moulding powder samples only. Impact hazard test: This test was the Rotter impact test 1A as described in the EMTAP Manual of Tests, issue 5, November 2016[14]. The Bruceton staircase procedure was used to establish median drop heights for the test material, and this was used to determine the Figure of Insensitiveness (FoI) value. Samples (30–40 mg) were placed in a concavity at the centre of the supporting frame of the Rotter test apparatus. A free-fall weight (5 kg) and striker were suspended above. The tests followed the Bruceton "up and down" testing technique with 50 replicates and the results were based on the height at which the compound was initiated 50 % of the time, with the mean height reported as the FoI. The FoI results were presented relative to RDX, where FoI> 80 indicates a material that is less sensitive than RDX, and FoI< 80 indicates a material that is more sensitive than RDX to impact initiation. Initiation was determined by the observation of parameters such as sound, smoke, flash and volume of gas released immediately after impact, and is therefore affected by operator judgment. **Electrostatic hazard test (ESD):** This test was the Electric Spark Test no. 6 as described in the EMTAP Manual of Tests, issue 5, November 2016. Test samples are subjected to discharges of 4.5, 0.45 and 0.045 J. Nylon spark test strips were filled with the material and sealed with copper tape. Up to 50 tests were performed at each of the three energy levels to determine a minimum spark energy that causes ignition. The samples were inspected for perforation or signs of decomposition. **Friction hazard test** This test was the Mallet Friction Test No. 2 as described in the EMTAP Manual of Tests, issue 5, November 2016. In this test a small sample (100 mm^3) of explosive is spread onto an anvil and struck a glancing blow with a standard wood or steel-tipped or nylon-tipped mallet held in the operator's hand. Results are reported as the number of ignitions occurring during ten cycles. **Thermal ignition hazard test** This test was the Temperature of Ignition Test No. 3 as described in the EMTAP Manual of Tests, issue 5, November 2016. In duplicate, small weighed quantities (200 mg) of the explosive under test are heated in borosilicate test tubes placed in a steel block, the temperature of which is controlled to rise at a steady rate (5 K min^{-1}), until an event occurs. For hand mixed propellant samples, a 10 shot (Langlie) method was used for impact, friction and ESD, due to less sample availability.

3 Results and Discussion

3.1 Performance calculation

The theoretical specific impulse of AP/SEBS propellant calculated using the ICT thermodynamic code compares well with a AP/HTPB propellant with values of 2473 N s kg^{-1} and 2480 N s kg^{-1} respectively, for 90 % w/w solids loading of AP (Figure 2). Similarly, an RDX/SEBS gun propellant compares well to RDX/HTPB with force constants of 1043 J g^{-1} and 1095 J g^{-1} respectively for a 84 % w/w solid loading of RDX. The difference in the specific impulse and force constants are relatively small. The HTPB propellant has higher calculated performance data because of its higher enthalpy of formation. This was expected as both binders are inert and mostly contain only hydrogen and carbon. We can conclude from this data that SEBS is a suitable alternative to HTPB as a propellant binder.

3.2 RAM slurry process optimisation (inert)

The influence of mixing at different G-forces and the flow rate of the anti-solvent was assessed on the propellant formulation process. For the purposes of processes development an inert filler of bimodal coarse (caster) and fine (icing) sugar was used. The ratio of the bimodal mixture of the sugars was the same as that later used for AP, however the particle size of the fine sugar was smaller than the equivalent fine AP used (Table 2. Particle size distribution for fillers, as determined by

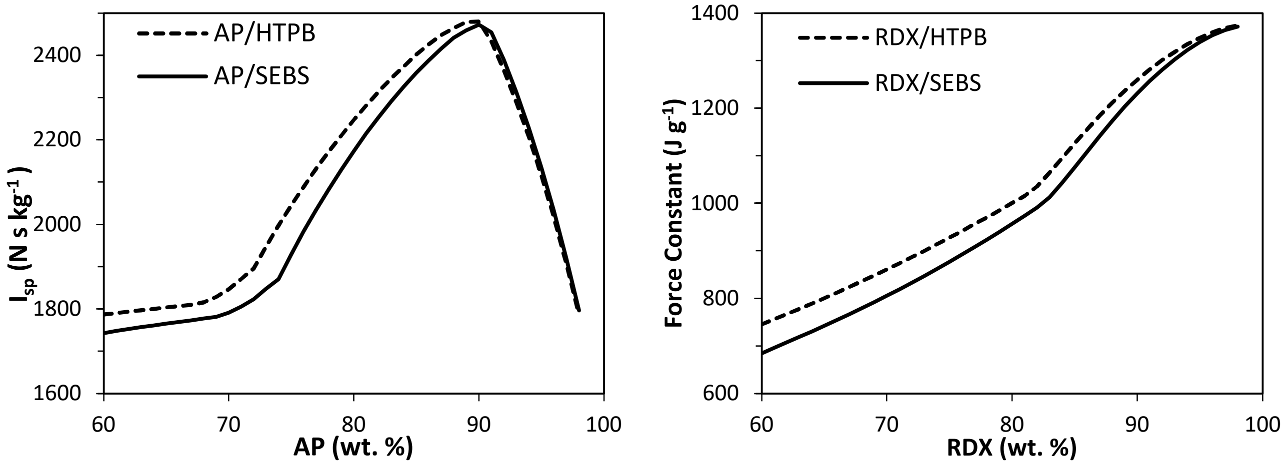

Figure 2 (left) Relationship of theoretical specific impulse (I_{sp}) against solid loading for AP/SEBS and AP/HTPB propellants. **(right)** Relationship of theoretical force constant against solid loading for RDX/SEBS and RDX/HTPB propellants.

laser diffraction using a Cilas 1190 in dry mode (sugar and AP) and wet mode (RDX). Despite the rheology of the inert sugar formulations being different to the live mixes, due to different particle morphologies (more angular), this was considered a reasonable guide for process development and optimisation. These inert mixtures were produced on a 10 g scale with 70 % w/w solid loading. Above 40 G acceleration the mixing was overly turbulent to be effective, and below 23 G the formulation was quiescence and did not mix.

Table 2. Particle size distribution for fillers, as determined by laser diffraction using a Cilas 1190 in dry mode (sugar and AP) and wet mode (RDX).

Filler	Diameter at 10 %, D_{10} (μm)	Diameter at 50 %, D_{50} (μm)	Diameter at 90 %, D_{90} (μm)
AP200	185	225	301
AP90	54	119	240
RDX class 5	10	24	45
Inert - caster sugar	191	254	374
Inert - icing sugar	3	16	27

Figure 3 shows that decreasing the acceleration from 40 to 23 G reduced the tap density by 13 % and the amount of fine material (<0.425 mm particle size) decreased from 30 % to less than 3 % w/w. The reduced tap density is due to the reduced fines reducing the packing efficiency of the propellant powder. The flow rate of the anti-solvent (at 25 G) has a lesser effect on the coating process. Decreasing the rate of addition from 6 to 1.5 cm^3 min^{-1} decreased the tap density by 10 %, and reduced the fine material from 11 % to <4 % w/w.

Optical microscopy (Figure 4) showed that the smallest fraction (<0.425 mm) contained uncoated crystals of the coarse filler. Conversely, the larger fractions (>0.425 mm) all contained well-coated agglomerates of the crystals, with some edges of the particles exposed at the surface.

The propellant moulding powder was produced on a larger scale (30 g), the procedure was based on data gathered from the inert process optimisation. It was shown that increasing the flow rate of anti-solvent increased agglomeration of the moulding powder. Therefore, the maximum flow rate (10 cm^3 min^{-1}) was

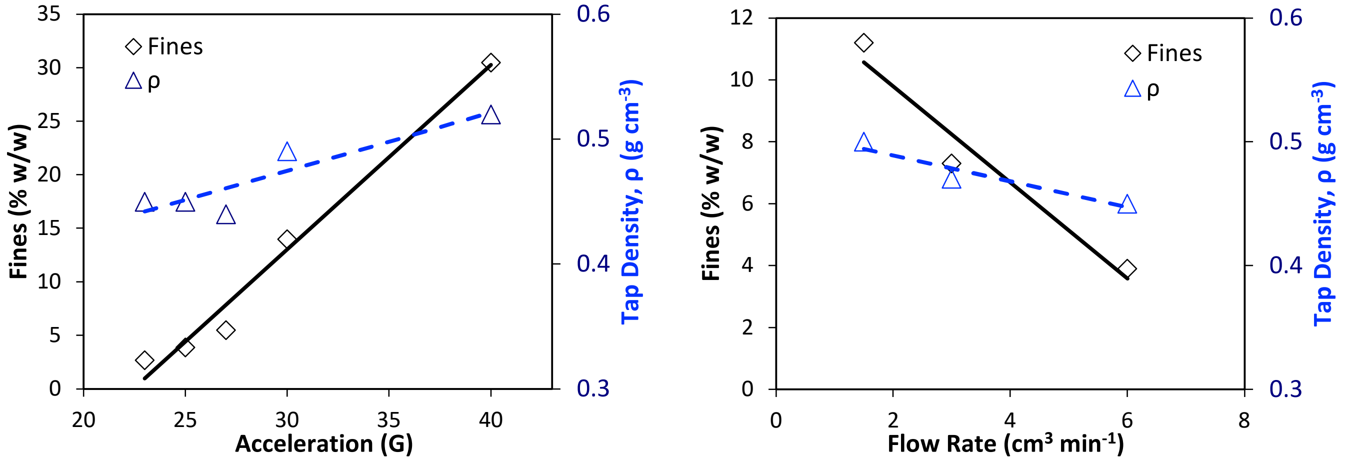

Figure 3. Slurry coating of inert moulding powder, fines (<0.425 mm particle size) percentage and tap density (ρ) as a function of **(left)** LabRAM acceleration (at 6 cm^3 min^{-1} flow rate) and **(right)** anti-solvent (IPA) addition (at 25 G).

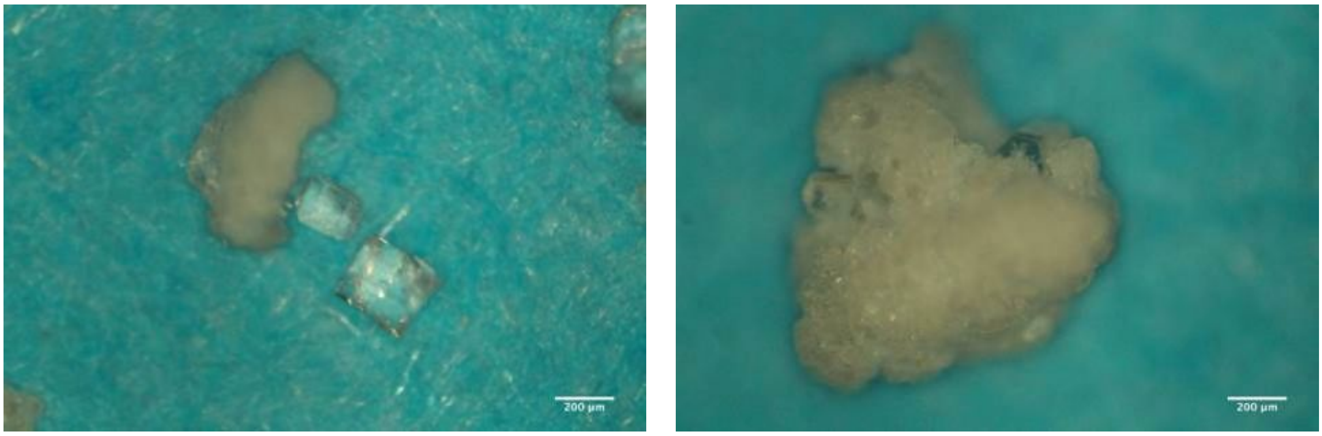

Figure 4. Optical images of inert moulding powder sieve fractions **(left)** < 0.425 mm fraction with uncoated filler and **(right)** < 0.425 mm fraction with a well-coated agglomerate example. LabRAM acceleration at 25 G during addition of anti-solvent (IPA) at 6 cm^3 min^{-1}. See supplementary data for more details.

Table 3. DSC compatibly testing of SEBS with AP and RDX. STANAG 4147 test 4[13]. See supplementary data (Figure S 1) for DSC thermograms.

Test Materials	Shift of 1st exothermic peak by DSC (T_d), mixture subtract explosive* (°C)	Peak Shape / Changes Observed	Compatible if shift in T_d < 4 °C
SEBS & AP	-0.54	Mixture has additional exothermic peaks at 348.3 & 358.5 °C.	Yes, but additional peaks may indicate incompatibility.
SEBS & RDX	+2.89	No changes.	Yes

*Test conditions: 2 °C min^{-1} heating rate, aluminium crucibles, N_2 sample atmosphere.

Table 4. Vacuum stability compatibly testing of SEBS with AP and RDX. STANAG 4147 test 1B[13].

Test Materials	Volume of gas from 5 g of mixture subtract volume of gas from 2.5 g of each component*, V_R (cm^3)	Compatible if V_R < 5 cm^3
SEBS & AP	0.14	Yes
SEBS & RDX	0.49	Yes

*Test conditions: 100 °C, 40 h.

used. The lower the rate of acceleration (to a minimum of 23 G) the better was the moulding powder agglomeration. For propellant scale up 30 G acceleration was chosen to optimisation agglomeration and ensure mixing was achieved.

3.3 Compatibility testing

Compatibility testing of the raw ingredients was conducted to evaluate the stability of the composite propellants being formulated. DSC compatibly testing (Table 3) on SEBS with RDX showed only a small shift (<4 °C) in peak temperatures of the first exotherm indicating. The SEBS with AP also showed a small shift, however there was an addition of a second exothermic peak in the AP/SEBS which is discussed later in section 3.6. Further assessment by vacuum stability (Table 4) yielded only a small increase in gas released (<0.5 cm^3) for both SEBS with RDX and AP, demonstrating the chemical compatibility of both mixtures.

3.4 Hazard testing

In line with novel propellant development protocols, small scale (10 g) hand mixed moulding powders were first tested before scale up to 30 g LabRAM. Hazard testing of the AP/SEBS propellants powders indicate that the hand mixed material produced a slightly more sensitive powder as tested by impact and friction, compared to the LabRAM materials. For instance, the Figure of Insensitiveness (FoI) for the AP/SEBs hand mixes were 39-45 compared to 60-73 for the LabRAM. Note: the hand mixed data is from Langlie-10 shot and the LabRAM used a 50-shot Bruceton, so a direct comparison is difficult. All the samples showed no ignition to the electric spark test (4.5J). Full results are in the supplementary data (Table S 1 & Table S 2). Comparing the AP-SEBS formulation the LabRAM mixing seems to produce a less sensitive material than the hand mixed moulding powder.

3.5 Density

The true densities for the pressed propellant found by gas pycnometry were in good agreement with the calculated theoretical maximum densities (TMD), see Table 6. Bulk densities obtained from hand measurement were in close agreement with each other. For AP/SEBS with a solid loading of 80 % w/w and lower, the bulk densities were consistently about 3 % lower than the TMD, indicating a small degree of porosity within the propellant. However, for the

Table 5. Hazard testing of hand and RAM slurry mixed propellant moulding powders.

Method	Samples	FoI [a]	Mallet friction [b]	Electric spark [c]
Hand Mixed	AP/SEBS (60 to 90 % AP)	39-45	Steel / Steel 0%	> 4.5J
RAM Slurry	AP/SEBS (60 to 84 % AP)	60-73	Steel / Steel 50%	> 4.5J
Hand Mixed	RDX/SEBS (60 to 90 % RDX)	42-44	Steel / Steel 50%	> 4.5J
RAM Slurry	RDX/SEBS (80/20)	39	Steel / Steel 50%	> 4.5J

[a] FoI - Rotter impact test, Langlie 10 shot (hand mixed) or 50 shot (RAM slurry), referenced to RDX (FoI 80), EMTAP 1A.
[b] EMTAP test 2. [c] EMTAP test 6, 10 (hand mixed) or 50 (RAM slurry)

Table 6. Density measurements of AP/SEBS and RDX/SEBS propellants. Duplicate analysis, standard deviation (σ) reported.

Sample	TMD (g cm^{-3})	True Density[a] (g cm^{-3})	Bulk Density[b] (g cm^{-3})	Bulk TMD (%)
AP/SEBS (60/40)	1.338	1.346 (σ = 0.014)	1.309 (σ = 0.030)	97.2
AP/SEBS (70/30)	1.452	1.444 (σ = 0.109)	1.410 (σ = 0.000)	97.7
AP/SEBS (80/20)	1.587	1.578 (σ = 0.040)	1.526 (σ = 0.017)	96.7
AP/SEBS (84/16)	1.648	1.675 (σ = 0.030)	1.525 (σ = 0.005)	91.1
RDX/SEBS (80/20)	1.516	1.493 (σ = 0.007)	1.419 (σ = 0.015)	93.6

[a] Helium gas pycnometry. [b] Hand measurements of samples.

84 % w/w loading the bulk density was almost 9 % lower than the TMD. An explanation for this is that this formulation is reaching the limit of binder/particle packing fraction and there isn't enough binder to complete coat and fill all the voids between the filler particles. Packing of monomodal spheres has a maximum packing fraction of 74 % v/v [15]. AP/SEBS (84/16) has a packing fraction of 71 % v/v. In reality, a lower maximum packing fraction is achieved due to the sphere packing arrangement being more random. On the other hand, having a range of distribution of particle sizes will increase the maximum packing fraction[1,15]. As expected, the mono-modal distribution of RDX packed less efficiently with a TMD of 93.6 % compared with the bimodal AP (96.7 % TMD).

3.6 Thermal analysis

TGA-DSC thermal analysis was performed on the AP based propellants and compared to pure AP. Looking at the DSC thermogram for pure AP (Figure 5 – left), there is an endothermic peak onset at 241 °C. This is well understood as an orthorhombic to cubic solid-solid phase transition [16,17]. Then follows an exothermic peak (295 °C) followed by another endothermic peak (418 °C). A two-step decomposition of AP is well known, although both of these should be exothermic with Zhu *et al*[18] seeing peaks at 330 and 434 °C. However, sublimation of the partially decomposed AP can occur, the resultant endotherm can then dominate over any remaining material undergoing the second decomposition [16]. If the sublimation effect is suppressed by, for instance, reducing the size of the

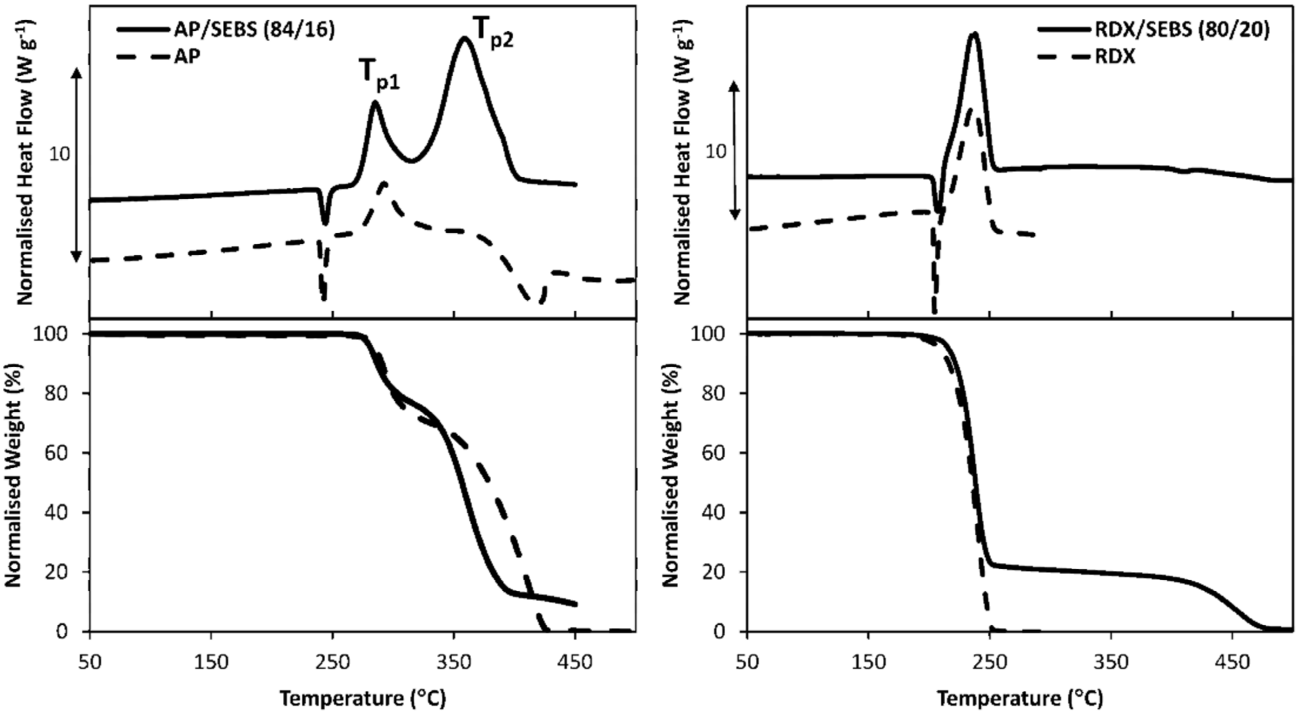

Figure 5. DSC **(top)** and TGA **(bottom)** thermograms for AP & AP/SEBS (84/16) propellant **(left)**, and RDX and RDX/SEBS (80/20) propellant **(right)**. Exotherms are represented by positive peaks. 10 °C min^{-1} heating rate under nitrogen. DSC traces have been shifted vertically for clarity.

hole in the lid of the crucible, then a second exotherm is seen[19].

The DSC thermogram of AP/SEBS (84/16), has the same endothermic peak (onset of 240 °C) as found with pure AP due to its solid phase transition. Then follows two exothermic peaks (T_{p1} & T_{p2}) with peaks at 288 & 362 °C. The first exothermic peak is very similar to the first decomposition peak found with pure AP, with a comparable onset and enthalpy. However, the second peak T_{p2} is a decomposition exotherm at a significantly lower onset than the dominant sublimation endotherm observed for pure AP. This is due to the combustion of SEBS with AP. This combustion reaction is known to occur between gaseous products of the AP decomposition and the binder [20] and has been studied by thermal analysis for AP/HTPB compositions [21]. The TGA thermograms provides further evidence of this two-step decomposition (Figure 5 - left).

The DSC and TGA results for different solid loadings of AP/SEBS propellants (Supplementary Data Table S 3 & Table S 4) are as expected. As the solid loading is increased more energy is expected to be released, this is shown be the increase in the enthalpy of decomposition. The phase change and first decomposition peaks remain reasonable unchanged, while the shape of the second decomposition peak changes causing the peak temperature to lower with increasing AP content, this provides further evidence for a reaction between the AP and SEBS.

The DSC thermogram of RDX/SEBS (80/20) propellant (Figure 5 - right) shows a very similar DSC thermogram to that of pure RDX, with the characteristic melting endotherm (onset 204 °C) followed by an exothermic decomposition (onset 216 °C). The shape of the curve has changed slightly with the endotherm not being as sharp as the pure RDX. The onset of decomposition has shifted by 3 °C degrees lower (to 213 °C) for RDX/SEBS (80/20) propellant compared to pure RDX, while the peak temperature has increased from 237 to 241 °C. This small difference may simply be physical. The enthalpy of decomposition is close to the expected value (about 5 % larger), when considering of the proportion of RDX in the composition. The TGA data also indicates separate decomposition for RDX and SEBS. By contrast, Abd-Elghany *et al* [22] showed the DSC peak value for decomposition of RDX/HTPB was 14.3 °C lower than pure RDX.

The apparent activation energy ($\boldsymbol{E_a}$) for decomposition for AP/SEBS (84/16) propellant was determined by DSC, using the Kissinger equation(1)[23]:

$$\boldsymbol{ln}\left(\frac{\beta}{T_p^2}\right) \cong -\frac{E_a}{R}\cdot\frac{1}{T_p} + \boldsymbol{ln}\left(\frac{AR}{E_a}\right) \tag{1}$$

where $\boldsymbol{\beta}$ is the heating rate of the DSC (°C min^{-1}), $\boldsymbol{T_p}$ is the peak temperature of the decomposition peak (°C), $\boldsymbol{E_a}$ the apparent activation energy (kJ mol^{-1}), $\boldsymbol{R}$ the molar gas constant (J K^{-1} mol^{-1}), and $\boldsymbol{A}$ is the pre-exponential factor (s^{-1}). Small samples of the propellant (ca. 5 mg) were analysed in triplicate at heating rates of 1, 2, 5 & 10 °C min^{-1}. The DSC thermograms (see supplementary data Figure S 4) contained two exothermic peaks, these were assigned as T_{p1} and T_{p2}. By plotting a graph of graph of $ln(\beta/T^2)$ against 1000/RT (Figure 6), the E_a can be obtained from the slope of the line. It was expected that the E_a obtained for the AP/SEBS (84/16) propellant would be close to that obtained for AP/HTPB propellants as both have hydrocarbon binders. However, the result reported by Gore *et al* [24] (188 & 251 kJ mol^{-1}) was substantially higher while the single result from Goncales *et al* [21] (126.2 kJ mol^{-1}) is much closer to E_a of the first peak. As Goncales *et al* conducted their experiment at faster heating rates, they only observed one exothermic peak. This is due to the first exothermic peak (peak 1) increasing in temperature with the increasing heating rate, causing it to join with the second exothermic peak (peak 2). Hence, their single E_a should be comparable to the 1st decomposition peak found for AP/SEBS.

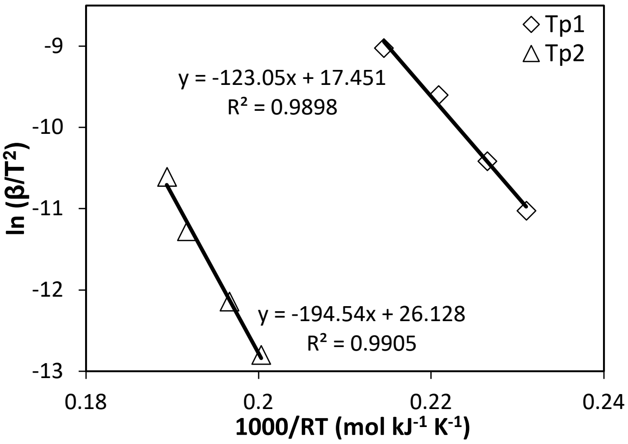

Sample	E_a for 1st Decomposition Peak, T_{p1} (kJ mol^{-1})	E_a for 2nd Decomposition Peak, T_{p1} (kJ mol^{-1})
AP/SEBS (84/16)	123.1	194.5

Figure 6. (top) Kissinger plot for AP/SEBS (84/16) propellant of the 1st (T_{p1}) and 2nd (T_{p2}) decomposition peaks. **(bottom)** Apparent activation energy for decomposition (E_a) of propellant found by DSC using the Kissinger method.

4 Conclusion

This research reports the formulation of a styrene-ethylene/butylene-styrene (SEBS), a commercially available off the shelf (COTS) thermoplastic elastomer (TPE), as a new propellant binder. The theoretical performance of AP/SEBS and RDX/SEBS propellants were calculated and found to be close to HTPB equivalent propellants. Both propellants were successfully manufactured with a fast and novel LabRAM slurry coating technique. Producing coated crystals that were easily processed into a propellant with appropriate density and hazard properties for gun and rocket propellants. Thermal analysis showed typical oxidiser behaviour of AP in the AP/SEBS propellant, while RDX showed little or no interaction with SEBS. The apparent activation energy for the decomposition of AP/SEBS by DSC was reported, this was similar to results obtained for AP/HTPB propellants.

Use of a thermoplastic elastomer binder would enable much easier removal and recycling of solid propellants, and using a commercial off the shelf binder provides cost and security of supply advantages. This work shows promise for the thermal and hazard properties of SEBS based propellants but does not address any of the mechanical properties. This being an important factor in the durability and safety of a propellant. Future work will address this, by accessing the mechanical properties of SEBS based propellants over a range of service and storage temperatures.

Acknowledgements

We would like to thank Cranfield University, in particular Prof Jackie Akhavan, for supporting this PhD. Thanks to the Cranfield - Test and Evaluation Group for the Hazard testing of the propellants. Daniel Jubb at The Falcon Project Ltd for his ongoing support and help with LabRAM formulation and development, and to Defence Equipment & Support (DE&S, UK MoD) for funding the procurement of the LabRAM at Cranfield University.

References

[1] G. P. Sutton, O. Bibarz, Solid Propellants, in: *Rocket Propulsion Elements*, Wiley, New Jersey, **2016**.

[2] J. A. Brydson, *Thermoplastic Elastomers - Properties and Applications, Rapra Review Reports*, Rapra Technology Ltd, Shrewsbury, **1995**.

[3] "Top Five Types of Industrial Mixing Equipment," **2021**, available at: https://resodynmixers.com/2021/02/01/top-five-types-of-industrial-mixing-equipment/ (accessed: 31st March 2021).

[4] S. L. Coguill, Synthisis of Highly Loaded Gelled Propellants, in: *AIChE Annual Meeting, At San Fransico CA, USA*, **2003**.

[5] Resodyn, "Energetic Mixing - Technical Paper," **n.d.**, available at: https://resodynmixers.com/technical-library/ (accessed: 26th June 2012).

[6] Resodyn, "Mixing Highly Loaded Polymers - Techical Paper," **n.d.**, available at: https://resodynmixers.com/technical-library/ (accessed: 4th April 2019).

[7] "RAM Technical White Paper," **2009**, available at: https://resodynmixers.com/ (accessed: 15th February 2010).

[8] D. J. Kasprzyk, D. A. Bell, R. L. Flesner, S. A. Larson, Characterization of a Slurry Process Used to Make a Plastic-Bonded Explosive, *Propellants, Explos. Pyrotech.* **1999**, *24*, 333–338, doi: 10.1002/(SICI)1521-4087(199912)24:6<333::AID-PREP333>3.0.CO;2-T.

[9] B. Olinger, *Compacting Plastic-Bonded Explosive Molding Powder to Dense Solids*, Report LA-14173, Los Alamos National Laboratory, New Mexico, USA, **2005**.

[10] J. Akhavan, T. C. Burke, Polymer Binder for High Performance Explosives, *Propellants, Explos. Pyrotech.* **1992**, *17*, 271–274, doi: 10.1002/prep.19920170602.

[11] D. G. Thompson, G. W. Brown, R. DeLuca, A. M. Giambra, M. M. Sandstorm, Thermal Expansion of PBX 9501 and PBX 9502 Plastic-Bonded Explosives, in: *Proceedings of the 37th Annual Conference of the North American Thermal Analysis Society, 21-23 September 2009*, Lubbock, TX, **2009**.

[12] M. A. Bohn, S. Cerri, Ageing Behaviour of Composite Rocket Propellant Formulations Investigated by DMA, SGA and GPC, *NDIA 2010 Insensitive Munitions Energ. Mater. Technol. Symp. "International Prog. Insensitive Munitions Energ. Mater.* **2010**, *Session 9*, 1–32.

[13] (NATO) North Atlantic Treaty Organization, *STANAG 4147 (Edition 2) - Chemical Compatibility of Ammunition Components with Explosives (Non-Nuclear Applications)*, NATO, Military Agency for Standardization (MAS), Brussels, **2001**.

[14] Defence Ordnance Safety Group, *EMTAP Manual of Tests Volume 1*, Ministry of Defence, London, **2016**.

[15] H. J. H. Brouwers, Particle-Size Distribution and Packing Fraction of Geometric Random Packings, *Phys. Rev. E - Stat. Nonlinear, Soft Matter Phys.* **2006**, *74*, 1–15, doi: 10.1103/PhysRevE.74.031309.

[16] S. Vyazovkin, C. A. Wight, Kinetics of Thermal Decomposition of Cubic Ammonium Perchlorate, *Chem. Mater.* **1999**, *11*, 3386–3393, doi: 10.1021/cm9904382.

[17] M. A. Sadek, M. H. Moeen, M. A. Radwan, H. H. Ameen, Effect of Aging on Thermal Decomposition of Ammonium Perchlorate, in: *32nd International Conferrence of ICT*, Karlsruhe, Germany, **2001**, pp. 129–1 to 192–12.

[18] Y. L. Zhu, H. Huang, H. Ren, Q. J. Jiao, Kinetics of Thermal Decomposition of Ammonium Perchlorate by TG/DSC-MS-FTIR, *J. Energ. Mater.* **2014**, *32*, 16–26, doi: 10.1080/07370652.2012.725453.

[19] R. I. Caro, Hyroxy-terminated polyether binders for composite rocket propellants, *PhD Thesis* **2006**, doi: 10.1057/978-1-349-95988-4_294.

[20] B. Gossant, Solid Propellant Combustion and Internal Ballistics of Motors, in: *Solid Rocket Propulsion Technology* (Ed.: A. Davenas), Pergamon Press, Oxford, **1993**.

[21] R. F. B. Goncalves, J. a F. F. Rocco, K. Iha, Thermal Decomposition Kinetics of Aged Solid Propellant Based on Ammonium Perchlorate - AP/HTPB Binder, *44th AIAA/ASME/SAE/ASEE Jt. Propuls. Conf. Exhib.* **2008**, 325–342, doi: 10.5772/52109.

[22] M. Abd-Elghany, A. Elbeih, S. Hassanein, Thermal Behavior and Decomposition Kinetics of RDX and RDX/HTPB Composition using Various Techniques and Methods, *Cent. Eur. J. Energ. Mater.* **2016**, *13*, 714–735, doi: 10.22211/cejem/64954.

[23] H. Kissinger, Reaction Kinetics In Differential Thermal Analysis, *Anal. Chem.* **1957**, *29*, 1702–1706, doi: 10.1021/ac60131a045.

[24] G. M. Gore, A. N. Nazare, C. N. Divekar, S. K. Hait, S. N. Asthana, Studies on Nonaluminized High Burning Rate AP-Composite Propellants, *J. Energ. Mater.* **2004**, *22*, 151–169, doi: 10.1080/07370650490522785.

Received: 14th May 2021
Accepted: 18th August 2022

Styrene-ethylene/butylene-styrene (SEBS) block copolymer binder for solid propellant

Wilkinson, Peter J.

2021-09-20

Wilkinson PJ, Weaver MC, Kister G, Gill PP. (2022) Styrene-ethylene/butylene-styrene (SEBS) block copolymer binder for solid propellants. Propellants, Explosives, Pyrotechnics, Volume 47, Issue 1, Paper number e202100142

https://doi.org/10.1002/prep.202100142